Visual Preference Modeling and Optimization in Graphic Design via Feature Encoding and Apriori Rule Mining

Yubin Wu[1], Juanping Kang[2*]
[1]School of Media and Art Design, Gui Lin University of Aerospace Technology, Guilin City, Guangxi Province, 541004, China
[2]Audit Office, Gui Lin University of Aerospace Technology, Guilin City, Guangxi Province, 541004, China
E-mail: Kjp2014guat@163.com
*Corresponding Author

Keywords: visual preference recognition, graphic design, feature encoding, apriori rule mining, cluster optimization

Received: August 9, 2025

Graphic design currently lacks computationally accurate methods for identifying and optimizing user visual preferences, hindering personalized and precise design outcomes. This paper presents a computational method integrating multidimensional feature encoding and Apriori rule mining to extract interpretable visual preference patterns from user feedback, enabling targeted design optimization. A multidimensional feature matrix encompassing color, layout, font, and graphic structure is constructed and encoded into a standardized preference dataset derived from 1280 user-selected design samples. The Apriori algorithm extracts high-confidence association rules linking visual element attributes to user preference outcomes, filtering representative combinations with minimum support 0.05 and confidence 0.6. Rule sets are vectorized to represent structured user group preferences, and a preference pattern map is generated via K-means clustering with five clusters, achieving an average silhouette coefficient of 0.63. High-confidence rules are embedded as constraints in an automated design generation module, reconstructing visual solutions aligned with user preferences, validated at 89.2% extraction accuracy under support threshold 0.09. Experimental validation confirms 89.2% preference extraction accuracy at support threshold 0.09 and silhouette coefficient 0.63 for five clusters, demonstrating effectiveness and adaptability in preference modeling and optimization.

Povzetek: Razvita je metoda za modeliranje vizualnih preferenc v grafičnem oblikovanju z večdimenzionalnim kodiranjem značilk in rudarjenjem asociacijskih pravil Apriori. Pravila se uporabijo za gručenje uporabnikov in optimizacijo oblikovalskih rešitev, kar omogoča razložljivo in podatkovno podprto prilagajanje oblikovanja.

1 Introduction

Existing research on rule extraction suffers from insufficient modeling capabilities and a lack of structured expression, making it difficult to systematically extract stable and interpretable visual preference rules from user feedback. This study aims to verify the effectiveness of association rule mining methods in modeling visual preferences in graphic design and proposes three core hypotheses. First, a multidimensional feature encoding system constructed based on user behavior feedback can effectively improve the Apriori algorithm's ability to extract high-confidence visual preference rules. Second, vectorizing and clustering high-confidence rules can generate a semantically interpretable map of user preference patterns. Third, embedding such rules into an automated design generation module can more stably output visual solutions that meet user preferences across cross-task scenarios compared to traditional feature dimensionality reduction or ensemble learning methods. The proposed method constructs a multidimensional visual feature matrix and combines it with user behavioral feedback to generate standardized preference labels. Then, the Apriori algorithm is used to mine high-confidence association rules, which are then vectorized and clustered to form a user preference pattern map. Finally, these rules are embedded in an automatic design element combination module for targeted reconstruction. This entire process, from data representation and rule mining to structure identification and result reconstruction, systematically addresses the shortcomings of existing research in modeling capabilities and structural representation, ensuring that the extracted preference rules are stable and interpretable, directly serving the design optimization goal. Faced with diverse user aesthetic preferences and complex media environments, traditional graphic design methods often rely on designers' subjective experience and lack systematic integration and quantitative analysis of user visual preference data [1], [2]. This approach struggles to provide targeted visual expression when faced with large-scale design demands or diverse user groups, resulting in a disconnect between design output and user perception [3], [4]. Existing research on summarizing design experience in graphic design visual elements has a

relatively mature cognitive system, but mapping user preference behavior data into computable visual patterns is still in the exploratory stage [5], [6]. At the same time, the increasingly diverse forms of user feedback on graphic design, such as ratings, click behavior, and browsing time, make extracting structural and pattern-based preference information from them a key challenge in current research [7], [8]. The lack of an effective feature encoding system limits the construction of a structural mapping relationship between user preferences and design elements, while the sparsity and interpretability of association rules further exacerbate the uncertainty in the process of visual preference pattern recognition [9], [10]. Therefore, establishing a computable feature model of design samples and systematically extracting stable preference patterns from user feedback to provide a basis for optimizing and recommending design elements has become a core issue in the current intelligent transformation of graphic design [11], [12]. The core contribution of this research lies in the construction of a complete technical chain from visual feature encoding to preference rule mining and design optimization. By structurally linking user behavioral feedback with multidimensional visual element attributes, a computational modeling of user visual preferences is achieved. This proposed method breaks through the limitations of traditional design, which relies on subjective experience and provides a data-driven personalized optimization framework for the graphic design field. This framework not only improves the accuracy of preference identification but also ensures the semantic interpretability of the extracted rules, thus supporting subsequent design generation and recommendation tasks. To address these issues, this paper introduces a rule-mining-driven visual element recognition and optimization method, focusing on the inadequate modeling and lack of structured expression in existing research on visual preference rule extraction. First, a visual element feature matrix encompassing multiple dimensions, including color type, layout form, font style, and graphic structure, is constructed and combined with user feedback to construct a standardized design preference dataset, ensuring data comparability in terms of dimensional consistency and category distinction. Furthermore, the Apriori association rule algorithm is used to mine patterns in the relationship between visual element attributes and user preference results, identifying effective rule sets with high support and confidence. The preference information is then transformed into structured input variables through rule vectorization. Subsequently, the KM clustering algorithm is used to group the rule vectors and generate preference pattern maps for different user groups, capturing the distribution patterns of group preference characteristics. Finally, the high-confidence rule set is embedded as a design logic constraint in the element automatic combination module, enabling personalized reconstruction and optimization of design results. This method integrates the entire process from design data characterization, preference information mining, and pattern structure recognition to visual result reconstruction, providing data support and a logical framework for the construction of intelligent design assistance systems. It has practical value and research significance in improving visual expression accuracy, user matching, and design solution optimization capabilities.

2 Related works

Existing research focuses on the mapping mechanism between visual elements and user behavior. However, in the context of graphic design, structuring the modeling of visual element attributes and user preferences remains a research difficulty. Pan et al. [13] proposed a personalized emotion recognition framework based on convolutional neural networks. By analyzing user facial expressions and visual elements of design works, they can accurately identify and classify emotional expressions in graphic design, thereby assisting designers to more effectively convey and stimulate the audience's emotional resonance. This focus on the user's emotional state provides technical support for understanding how design works to trigger visual feedback. Kong et al. [14] combined design principles with a data-driven ranking model to build an automated suggestion system for graphic design aesthetic optimization. They used learned human aesthetic preferences to evaluate and optimize the generated candidate solutions, thereby improving the efficiency and quality of the design process. This method emphasized the feasibility of iterative improvement based on existing designs. Gbadegbe et al. [15], based on the expectancy value theory and Bronfenbrenner ecosystem theory, used a quantitative research method to analyze the factors affecting the graphic design preferences of 340 visual arts students in Ghana, revealing how personal motivation, design ecosystem, and multiple attributes jointly drive students to choose graphic design. This study, drawing from an educational context, expands understanding of the mechanisms underlying design preference formation. However, none of these studies delve into the complexity and uncertainty inherent in modeling visual preferences due to individual differences.

These studies have made some progress in emotion recognition and aesthetic optimization, but they often focus on modeling user perception and lack a systematic exploration of the structural connections between design elements and preferences. Particularly in the context of graphic design, a computational modeling framework for mapping the combination of visual elements to user preferences has yet to emerge, making it difficult to effectively implement design optimization tasks.

In the area of rule mining methods and their application in design optimization, existing research has explored multiple levels of algorithm improvement and cross-domain transfer. Liao S et al. [16]conducted clustering and association rule mining on survey data from 2011 Taiwanese TikTok users to generate user profiles and identify social interaction patterns, providing evidence that TikTok transcends traditional social media development paradigms. Li Y et al. [17] proposed the MCoR-Miner algorithm for maximal co-occurrence nonoverlapping sequential rule mining using depth-first search and indexing mechanisms, demonstrating superior efficiency and recommendation performance compared to

existing methods. In addition, Akgul et al. [18] combined fuzzy language summarization with genetic algorithms to extract fuzzy rules between emotional needs and product design form elements, and verified its effectiveness by comparing it with the results of fuzzy association rule mining, providing an operational technical path for the systematic transformation of emotional needs in complex product design. This method extends rule mining from structured data to the mapping relationship at the semantic level. However, these studies have largely focused on improving algorithmic performance or discovering rules in specific domains, but have not adequately addressed the complex aesthetic relationships between visual elements and the dynamic evolution of user preferences in the context of graphic design. Currently, there is a lack of rule mining methods specifically tailored to graphic design tasks to extract structured visual preference rules from user behavioral feedback, nor is there a rule-driven modeling system for design optimization.

3 Visual preference recognition and rule modeling methods

3.1 Construction of feature coding for graphic visual elements

Visual preference modeling is based on the structured expression of design features. The study constructs a multi-dimensional joint feature vector system to quantify the visual attributes of graphic design samples in terms of color, layout, font, and graphic structure. The color dimension is represented by the HSV (Hue, Saturation, Value) color space, and the ratio vector is constructed based on the pixel density of the main color distribution [19], [20], $C=[c_1,c_2,...,c_k]$, where c_k is the proportion of the (x_c,y_c) color kth categories [21], [22], and the sum is 1.

$$L_b=\sqrt{(x_c-x_0)^2+(y_c-y_0)^2} \tag{1}$$

(x_0,y_0) is the coordinate of the center point of the image. The graphic structure dimension constructs a compactness index through the contour geometry ratio:

$$G_c=\frac{A_g}{A_b} \tag{2}$$

A_g is the actual area of the graphic, and A_b is the area of the minimum enclosing rectangle. Font style extraction uses a pretrained convolutional neural network to extract embedding vectors. Principal component analysis (PCA) is then used to reduce the dimensionality of the font to generate a fixed-length high-dimensional representation, $F=[f_1,f_2,...,f_m]$, where m represents the number of dimensions after dimensionality reduction. The final unified visual feature vector has one hundred ninety two dimensions, composed of three color ratio components, one layout offset value, one graphic compactness value, and one hundred eighty seven dimensions from the PCA-reduced font embedding.

The above-mentioned encodings are concatenated to form a unified visual feature vector, $V=[C,L_b,\mathrm{F},G_c]$, which is used to represent the visual feature structure of a single design sample. Table 1 shows the schematic structure of the sample encoding, demonstrating the numerical representation of each attribute in a unified format:

Table 1: Multidimensional visual feature encoding of design samples

Sample ID	Color vector C main color ratio	Layout offset L_b	Graphics compactness G_c
S01	[0.41, 0.35, 0.24]	0.126	0.782
S02	[0.22, 0.55, 0.23]	0.294	0.605
S03	[0.48, 0.31, 0.21]	0.102	0.863
S04	[0.36, 0.28, 0.36]	0.189	0.712
S05	[0.33, 0.46, 0.21]	0.275	0.643

In Table 1, the color ratio vector, layout offset, and graphic compactness are presented in specific numerical form. The font style features are extracted through a pre-trained convolutional neural network and reduced in dimension by PCA to form a high-dimensional embedding vector, which is not listed in Table 1 due to its high dimension. This visual feature vector fully covers the four-dimensional attributes of color, layout, font, and graphic structure, with a total dimension of 192. Among them, the font dimension contributes 187 dimensions after principal component analysis compression, forming a standardized data structure for subsequent association rule mining.

All samples form a feature matrix $X\in\mathrm{R}^{n\times d}$, where n represents the number of samples, and d represents the number of feature dimensions for each sample. This matrix serves as the basic data interface for subsequent preference modeling and rule mining, ensuring numerical alignment and structural adaptation between the encoding and model layers.

3.2 User behavior data and visual preference label generation

The generation of user visual preference labels uses behavioral feedback data as input, constructing a structured preference mapping system to support subsequent rule learning tasks. The original behavior data matrix is denoted as $R=r_{ij}^{(k)}$, where $r_{ij}^{(k)}$ represents the response value of user i to the design sample j on the behavior dimension of category k. To unify the numerical scale of each type of feedback, the range normalization method is used to independently standardize each type of feedback [23], [24]. The normalization result is defined as:

$$\hat{r}_{ij}=\frac{r_{ij}-min(r_i)}{max(r_i)-min(r_i)} \tag{3}$$

$max(r_i)$ and $min(r_i)$ represent the maximum and minimum values of all feedback from the user i, and $\hat{r}_{ij} \in [0,1]$.

Each element in the original behavioral data matrix represents a specific user's response to a specific behavioral dimension of a designed sample. To ensure numerical comparability across different feedback types, range normalization is used to independently normalize each type of feedback. The normalized results serve as input to a weighted fusion model, which combines three types of feedback: clicks, ratings, and dwell time, to generate a single, comprehensive preference score. This process transforms multi-source, heterogeneous behavioral signals into a unified numerical representation, providing a stable and semantically clear supervisory variable for subsequent association rule mining. After the multi-source behavior signals are normalized, a weighted fusion model is used to generate a comprehensive preference score [25], [26], denoted as s_{ij}, which is calculated as follows:

$$s_{ij}=\alpha\cdot\hat{r}_{ij}^{(1)}+\beta\cdot\hat{r}_{ij}^{(2)}+\gamma\cdot\hat{r}_{ij}^{(3)},\alpha+\beta+\gamma=1 \quad (4)$$

$\hat{r}_{ij}^{(1)}$, $\hat{r}_{ij}^{(2)}$, and $\hat{r}_{ij}^{(3)}$ are the normalized results of click, rating, and duration feedback, respectively. $\alpha+\beta+\gamma=1$ and $\alpha,\beta,\gamma\in[0,1]$ are empirical weight parameters. The weight parameters α and β are set based on empirical research on the relative contribution of multi-source behavioral signals in visual preference prediction. Clicking behavior and rating behavior have a high consistency in expressing user preferences, while the explanatory power of dwell time as implicit feedback is slightly lower [27]. Through cross-validation and grid search, the parameter space is optimized, and α is finally determined to be 0.4 and β to be 0.3 to maximize the correlation between preference labels and users' actual choice behavior. This configuration remains stable on multiple independent datasets, ensuring the generalization ability of the fusion model in different scenarios. Table 2 lists the standardized behavior values and final scores of some users in different dimensions:

Table 2: Normalization of user behavior feedback and preference scores

User ID	Click normalization	Score normalized	Duration normalized	Overall preference score s_{ij}
U01	0.82	0.67	0.75	0.743
U02	0.45	0.51	0.48	0.480
U03	0.91	0.76	0.82	0.853
U04	0.63	0.69	0.65	0.660
U05	0.27	0.34	0.30	0.305

In Table 2, the raw user feedback, after normalization and weighted fusion, has clear distribution boundaries, allowing for precise mapping to preference labels. This process not only establishes a signal foundation for preference discrimination but also ensures the semantic stability and numerical rationality of the label dataset. This provides clear supervisory variables for Apriori rule mining and ensures that the rule results are consistent with behavioral responses.

Preference labels are generated based on the aforementioned scoring results, which are converted to a discrete binary form using a threshold function. Setting the global preference boundary parameter θ, the label generation function is defined as:

$$y_{ij}=\begin{cases}1, & s_{ij}\geq\theta\\ 0, & s_{ij}<\theta\end{cases} \quad (5)$$

$y_{ij}\in0,1$ indicates whether user i exhibits a positive preference for sample j. This preference label is aligned with the sample feature vectors one by one to construct a training dataset $D=(x_j,y_{ij})$, which supports subsequent high-confidence visual rule association mining. This encoding strategy ensures numerical consistency in behavioral feedback data and clear discriminant boundaries for labeling, enhancing the model's adaptability for extracting preference patterns.

3.3 Apriori-based visual element-preference association rule mining

Uncovering the potential correlation patterns between visual features and user preferences is a key step when building a design preference modeling mechanism. Let the feature vector of a design sample be $x_j\in R^d$, and its corresponding user preference label be $y_{ij}\in0,1$. The two are combined to form the labeled training sample set $D=(x_j,y_{ij})$. To map continuous-valued features to discrete item sets, a symbolic encoding operation $\phi:R^d\rightarrow I^k$ is constructed to project sample features onto a discrete attribute set I. This allows each sample to consist of a set of attribute items, forming a transaction item set T_j, satisfying the input format requirements of the Apriori algorithm.

The frequent item set F is defined as the attribute combination set, whose frequency in the preference positive example set is greater than the minimum SC σ [28], [29], expressed as:

$$F=\{I\subseteq I|\frac{|\{T_j|I\subseteq T_j\wedge y_{ij}=1\}|}{|\{T_j|y_{ij}=1\}|}\geq\sigma\} \quad (6)$$

Based on the frequent item sets, the generated association rule is in the form of $I\Rightarrow y_{ij}=1$, where I is the combination of visual elements, and the latter is the preference expression. The confidence of the rule is defined as:

$$\text{conf}\,(I \Rightarrow y_{ij}=1)=\frac{|\{T_j | I \subseteq T_j \wedge y_{ij}=1\}|}{|\{T_j | I \subseteq T_j\}|} \quad (7)$$

Rule filtering relies on a confidence threshold, retaining rule sets that satisfy conf greater than or equal to the confidence threshold [30]. Due to the exponential growth of the attribute item set space, a layered expansion and pruning strategy is employed to improve computational efficiency. Pruning is based on the Apriori principle: if the item set I is infrequent, then any superset of it is also infrequent, thus avoiding unnecessary computation.

3.4 Visual preference pattern discovery and user clustering

To achieve structured modeling of visual preference rules at the user level, a set of high-confidence rules needs to be vectorized, and a user-rule response matrix needs to be constructed as the basis for clustering. Each rule r_k corresponds to a visual element combination $a_1,a_2,...,a_s$, which is mapped to the complete set of discrete attributes I. A binary indicator vector $r_k \in 0,1^{|I|}$ is constructed, where $r_k[i]=1$ indicates whether attribute i belongs to rule r_k and is zero otherwise. After vectorizing all rules, it can obtain the rule encoding matrix $R \in 0,1^{m \times |I|}$.

Algorithm 1: Rule vectorization and constraint filtering for visual preference optimization.

Input: High-confidence association rule set R = {r₁, r₂, ..., rₙ},
Discrete attribute space A = {a₁, a₂, ..., aₘ},
Candidate design sample set D = {d₁, d₂, ..., dₖ}

Output: Filtered design candidate set D' ⊆ D,
Rule activation matrix V ∈ {0,1}^{n×k}

1: Initialize V as zero matrix of size n × k
2: for each rule $r_i \in R$ do
3: Construct binary indicator vector $v_i \in \{0,1\}^m$
4: for each attribute $a_j \in A$ do
5: if a_j is contained in r_i then
6: $v_i[j] \leftarrow 1$
7: else
8: $v_i[j] \leftarrow 0$
9: end if
10: end for
11: Store v_i as row i in V
12: end for

13: Initialize D' ← ∅
14: for each design sample $d_l \in D$ do
15: Compute response vector $s_l \in \{0,1\}^n$
16: for each rule $r_i \in R$ do
17: if d_l satisfies all attributes in r_i then
18: $s_l[i] \leftarrow 1$
19: else
20: $s_l[i] \leftarrow 0$
21: end if
22: end for
23: if sum(s_l) ≥ 1 then
24: Append d_l to D'
25: end if
26: end for

27: Return D', V

Based on this, the paper defines a rule activation vector $\mathbf{z}_i \in R^m$ for each user u_i. Its kth dimension represents the probability response value z_{ik} that the user satisfies rule r_k, calculated as follows:

$$z_{ik}=\frac{|\{j | r_k \subseteq T_j \wedge y_{ij}=1\}|}{|\{j | y_{ij}=1\}|} \quad (8)$$

T_j is the set of discrete attribute items of sample j, and $y_{ij}=1$ represents the preference expressed by user i for sample j. By traversing the rule hits of all preferred samples, the complete set of user rule vectors $Z=[\mathbf{z}_1^\top,\mathbf{z}_2^\top,...,\mathbf{z}_n^\top]^\top \in R^{n \times m}$ is obtained, which serves as the basis for expressing the preference structure space.

To identify the distribution pattern of user preference structure in the rule subspace, the KM algorithm is introduced to perform unsupervised clustering of Z. The objective function is to minimize the sum of the squared Euclidean distances from each sample to its corresponding cluster center, expressed as:

$$L_{\text{kmeans}}=\sum_{i=1}^{n} //\mathbf{z}_i-\boldsymbol{\mu}_{c(i)}//^2 \quad (9)$$

$\boldsymbol{\mu}_{c(i)}$ is the center vector of the cluster $c(i)$ to which user i belongs. By iteratively optimizing cluster centers and sample allocation, users in the same cluster maintain high consistency in their rule response structure. After cluster modeling, a user preference pattern map $P=C_1,C_2,...,C_K$ is obtained, where each cluster C_k consists of a group of users with similar distribution in the rule vector space. This structure supports subsequent design optimization, recommendation strategy embedding, and pattern consistency assessment based on preference type. Figure 1 illustrates the preference pattern modeling process based on rule vectorization and user clustering.

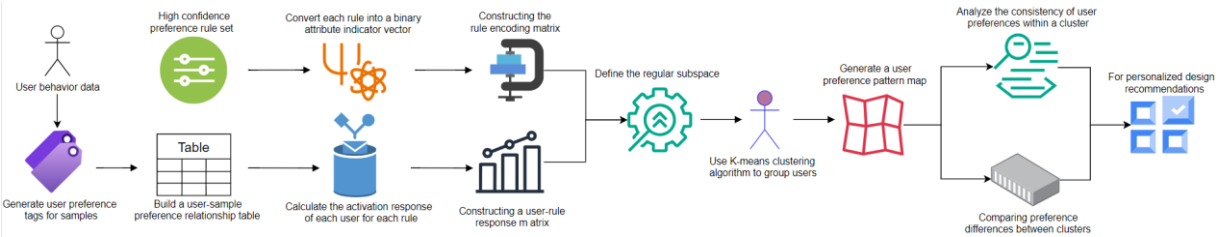

Figure 1: Preference pattern modeling based on rule vectorization and user clustering

Figure 1 shows the process of constructing a rule encoding matrix by converting high-confidence preference rules into binary attribute indicator vectors. Simultaneously, preference labels for the designed samples are generated based on actual user behavior data. Each user's activation response to each rule is further calculated to form a user-rule response matrix. Subsequently, the KM clustering algorithm is used within the rule subspace to group users and generate a visual preference pattern map. This map can be used to analyze the consistency of user preferences within a group and the differences in preferences between different groups.

3.5 Visual element combination optimization and generation

After completing preference rule mining and user pattern identification, a design generation mechanism with constraint control capabilities must be constructed to ensure that the design solution's visual attribute structure is highly consistent with high-confidence preference rules. This mechanism guides the generation of candidate design samples by converting rule sets into combined constraints and outputs the final optimization results based on feasibility screening and polynomial scoring sorting. Figure 2 shows the structural process of the design optimization mechanism driven by preference rules.

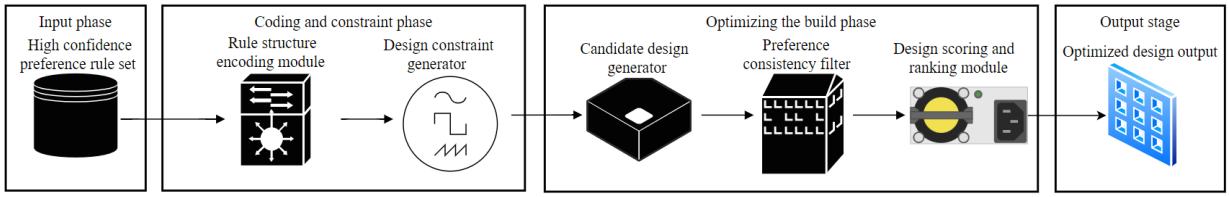

Figure 2: Preference rule constraint-driven design optimization mechanism

In Figure 2, a set of high-confidence rules is first structured and encoded to generate logical templates recognizable by the constraint system. This template then serves as the basis for constructing the conditional space for design generation. Candidate design solutions are then combined and generated based on the rule constraint logic. A preference consistency filter is then used to eliminate structurally non-compliant samples. The scoring module ranks and evaluates the filtered design set, ultimately outputting the optimal design solution that conforms to the preference rule structure. This architecture uses rules as logical input and embeds semantic knowledge into the design generation process, ensuring that the output solution is highly consistent with user preferences at the visual attribute level.

The set of high-confidence preference rules is denoted as $R=r_1,r_2,...,r_m$. Each rule r_k consists of a set of visual element attributes, which are encoded and mapped into a formal logic vector through the rule structure. The design constraint generator defines a response function $\Psi(\mathbf{s}_t,r_k)$ for each rule based on this logic template, where the value is 1 if the candidate design $\mathbf{s}_t$ satisfies the visual configuration in rule r_k, and 0 otherwise:

$$\Psi(\mathbf{s}_t,r_k)=\begin{cases}1, & \text{If design } s_t \text{ Satisfy the rules } r_k\\ 0, & \text{otherwise}\end{cases} \tag{10}$$

Based on this response function, a multi-rule weighted scoring model is defined to evaluate the preference fit of candidate design solutions:

$$J(\mathbf{s}_t)=\sum_{k=1}^{m}\boldsymbol{\alpha}_k\cdot\Psi(\mathbf{s}_t,r_k) \tag{11}$$

The confidence weight of the $\boldsymbol{\alpha}_k$ in rule r_k represents the structural importance of the rule in the preference distribution. A candidate design sample set is dynamically constructed from the visual element attribute space using a stratified sampling strategy. The number of samples is adaptively adjusted based on the coverage of the constraint rules, ensuring efficient exploration of the solution space while satisfying high-confidence preference rules. This strategy avoids enumerative exhaustive search to improve computational efficiency. Unlike black-box methods such as generative adversarial networks, it maintains an explicit connection between the generation process and the rule logic. The generated candidate set undergoes consistency filtering and then enters the scoring and ranking phase, ultimately outputting the optimal solution. The sample generator constructs the candidate set $\mathbf{s}_1,\mathbf{s}_2,...,\mathbf{s}_T$ from the design space S, and then uses the consistency filter to eliminate samples that do not meet the preference response threshold τ:

$$\mathbf{S}_{\text{valid}}=\left\{\mathbf{s}_t\in S\,\middle|\,\sum_{k=1}^{m}\Psi(\mathbf{s}_t,r_k)\geq\tau\right\} \tag{12}$$

Finally, the design with the largest score is selected from the samples that meet the response constraints as the final optimization output:

$$\mathbf{s}^*=\arg\max_{\mathbf{s}_t\in\mathbf{S}_{\text{valid}}}J(\mathbf{s}_t) \tag{13}$$

This mechanism achieves a combined optimization of rule-driven structural control and scoring-driven optimization, ensuring both logical consistency and preference matching when outputting visual design results. This creates a complete closed-loop from rule mining to automated optimization generation.

4 Experimental setup and implementation process

4.1 Planar visual element dataset construction and experimental configuration

The dataset contains 1,280 graphic design samples from commercial visual communication and digital media content, covering advertisements, brand logos, publication covers, and social platform interfaces. The visual element attributes, such as main color distribution, layout

structure, font style, and graphic composition, are all structurally annotated. User feedback is collected via offline platforms and web interactions, with all data anonymized to ensure participant privacy during processing. In the experimental data construction stage, the study collects a graphic design dataset for visual preference modeling based on commercial visual communication (covering commercial advertising, brand identity design, publication covers, etc.) and digital media content (covering social platforms, data visualization, etc.). The total number of image samples is 1,280, covering core dimensions, such as main color, typesetting, font style, and graphic composition. Each type of graphic visual element attribute constructs an attribute label system, and all samples complete the visual feature structured annotation. User feedback data comes from offline test platforms and web-based interactive behaviors. The collected indicators cover the design selection click frequency, dwell time, and explicit rating values. After normalization and conflict elimination, user preference mapping labels are generated, and a preference record matrix corresponding to the sample set is established. The platform hardware configuration is a dual-core Xeon processor with 128GB of memory and an RTX A6000 graphics card. The software development environment is Python 3.10. Data processing and algorithm training are deployed in TensorFlow 2.13 and Scikit-learn 1.4 environments, respectively.

4.2 Visual preference rule training and optimization task process

During the model training and task execution phases, this study uses a unified preference modeling and rule-driven optimization process, completing a closed-loop design from visual sample input to optimization output. The model training phase uses the pre-processed 192-dimensional sample input matrix as a foundation, loading visual feature vectors and user preference labels, and constructing a mapping space between visual attributes and behavioral labels. Based on this, the Apriori rule mining algorithm constructs frequent item sets and confidence matrices. Minimum support and minimum confidence serve as constraint thresholds to dynamically adjust the rule selection process, ultimately forming a complete set of rules. The rule set is then vectorized and clustered, mapped to the corresponding user group index, and the modeling of the multi-preference subset distribution structure is realized. To ensure that the generated solution strictly matches the user preference rules, the system builds a design optimization engine based on preference constraints. Its core strategy is to introduce a logical condition verification mechanism when generating design candidates. All candidate outputs must meet the structural conditions of at least one set of high-confidence preference rule items. To clarify the process of task and parameter configuration at each stage, Table 3 shows the key task parameter composition during the training phase and optimization engine initialization process.

Table 3: Preference rule model training and design optimization task configuration parameters

Stage	Input data dimensions	Total sample size	Core operating procedures	Parameter settings
Data loading	192	1280	Read visual feature vectors and preference labels	Batch size: 128, Loading method: Memory mapping
Rule mining	192	1280	Constructing frequent itemsets and confidence matrices	Minimum support: 0.05, minimum confidence: 0.6
Rule filtering	-	894	Filter weakly correlated rules to generate high-confidence rule sets	Redundancy threshold: 0.15, maximum itemset length: 5
Rule vectorization encoding	-	1280	Converting rule sets into structured vector representations	Encoding method: sparse matrix mapping, dimension compression: no
Preference-constrained optimization engine	192	Dynamic	Embedded logic matching mechanism for solution generation and filtering	Matching strategy: minimum coverage, number of execution threads: 4

As shown in Table 3, frequent item set generation and high-confidence rule screening constitute the bulk of the rule mining phase, determining the size of the constraint space for the subsequent optimization engine. The rule vectorization step implements the structural expression of preference logic, providing precision support for clustering and optimization. The optimization engine configuration parameters in the final phase directly impact design generation efficiency and preference coverage. This structure ensures logical continuity and parameter control throughout the entire task chain, ensuring consistent functional coupling between objectives at each stage.

During the rule mining phase, the maximum item set length is set to 5, and the redundancy threshold is set to 0.15, aiming to balance the expressiveness of the rule structure with generalization performance. Excessively long item sets can lead to sparse rule coverage, reducing

cross-scenario adaptability; excessive redundancy weakens the discriminability between rules and affects the accuracy of identifying user preference patterns. This parameter combination, through multiple rounds of cross-validation, maintains a high-confidence rule set size while ensuring that the generated rules have clear semantic boundaries, avoiding overfitting to specific behavioral data and losing the universal explanatory power of visual element combination patterns.

This process maintains the consistency of preference logic in the training and generation stages, ensures the user fit and rule interpretation ability of the output results, and provides a basic comparison structure for subsequent generalization verification.

5 Experimental results analysis and preference recognition evaluation

5.1 Evaluation indicators for visual preference rule extraction

In the performance analysis stage of visual preference rule extraction, to comprehensively evaluate the performance differences of this method in actual design tasks, the recognition effects of five different rule mining and feature modeling strategies under multiple SCs are compared. The processing logic of various methods in preference modeling is essentially different. Among them, PCA and Information Gain (IG) methods focus on screening preference dimensions from the perspective of dimension compression and feature importance; Random Forest (RF) method uses an integrated tree structure to build an attribute selection scoring mechanism; FP-Growth (Frequent Pattern Growth) directly mines potential common structures from the candidate set scale expansion items. The method in this paper combines visual encoding and Apriori logic rule screening, and uses user behavior-driven preference labels as supervisory variables to construct a multidimensional item set mapping mechanism, thereby improving rule coverage and semantic accuracy. The evaluation indicators use precision and recall to characterize the performance of preference determination, while the number of rules and average confidence are used as indicators of structural integrity and credibility. Figure 3 shows the comparison of the preference rule extraction performance of each method under different SCs. Notes: N represents the number of rules; C represents the average confidence; P represents precision; R represents recall.

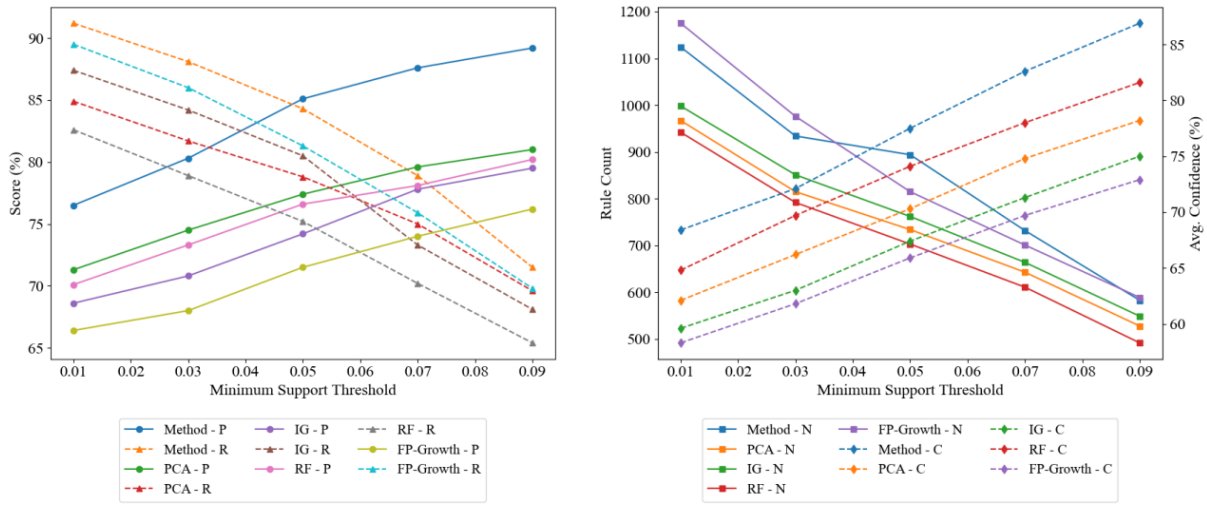

Figure 3: Comparison of preference rule extraction performance of various methods at different SCs

In Figure 3, as the SC increases from 0.01 to 0.09, the precision of the proposed method steadily increases from 76.5% to 89.2%, demonstrating a consistent trend of high-confidence rule sets enhancing preference accuracy. In contrast, the PCA method achieves a final precision of only 81.0%, and its recall decreases from 84.9% to 69.6%, indicating that the dimensionality compression process interferes with the identification of preference boundaries. The FP-Growth method shows a high recall rate in the low support range, reaching 89.5% at 0.01. However, as the SC increases, the confidence increases slowly, and the number of rules drops sharply to 589, reflecting its lack of a structural compression mechanism for rule generalization ability.

The proposed method extracts 894 high-confidence rules at 0.05 support, with an average confidence of 77.5%, which is much higher than 70.3% and 67.4% of PCA and IG, respectively. This is mainly attributed to the fact that the proposed method introduces a behavior-driven supervision strategy in the rule generation stage, enabling the rules to have stronger user-perceived matching capabilities. Based on the above indicators, the proposed method consistently maintains a leading trend within the support range, validating its optimization advantages in designing visual preference modeling.

Based on the above indicators, the proposed method continues to maintain a leading trend within the support range. Its optimization advantage comes from the fact that the behavior-driven supervision strategy strengthens the semantic mapping between visual element combinations and user preferences in the rule generation stage, avoiding the loss of key perceptual information in the unsupervised dimensionality reduction process. At the same time, the discretized attribute space and the frequent itemset

pruning mechanism synergistically improve the structural generalization ability of high-confidence rules.

5.2 Evaluation of visual preference group clustering

After extracting high-confidence preference rules, the study further models and analyzes the group structure of users in the rule response space. The selection of K-Means for clustering is grounded in its computational efficiency and interpretability within the context of this study's structured rule vector space. The cluster number k is determined by maximizing the average silhouette coefficient across a range of candidate values from three to seven. This metric evaluates intra-cluster cohesion and inter-cluster separation, providing an objective criterion for identifying the optimal partitioning that best reflects the underlying structure of user preference patterns within the rule response space. The rule vectors derived from Apriori mining are inherently discrete and sparse, forming a feature space where centroid-based partitioning aligns with the objective of identifying distinct, interpretable preference groups. Alternative density-based or hierarchical methods often require parameter tuning sensitive to data distribution or produce less intuitive cluster boundaries, which may obscure the direct mapping between rule sets and user segments essential for subsequent design optimization. K-Means provides a stable, deterministic outcome suitable for integrating into the constraint-driven generation pipeline, ensuring consistent cluster assignments across iterations necessary for evaluating recommendation performance. To verify the impact of different modeling approaches on user clustering, user response matrices are constructed based on the five feature extraction strategies described above, and the KM clustering algorithm is uniformly used for multi-clustering. The average silhouette coefficient and the Davies-Bouldin Index (DBI) are used as the primary indicators in the evaluation process. The former reflects intra-cluster consistency, while the latter measures inter-cluster separability, comprehensively characterizing the rationality of the cluster structure and the clarity of its boundaries. Figure 4 shows the trends of these two indicators for different cluster numbers.

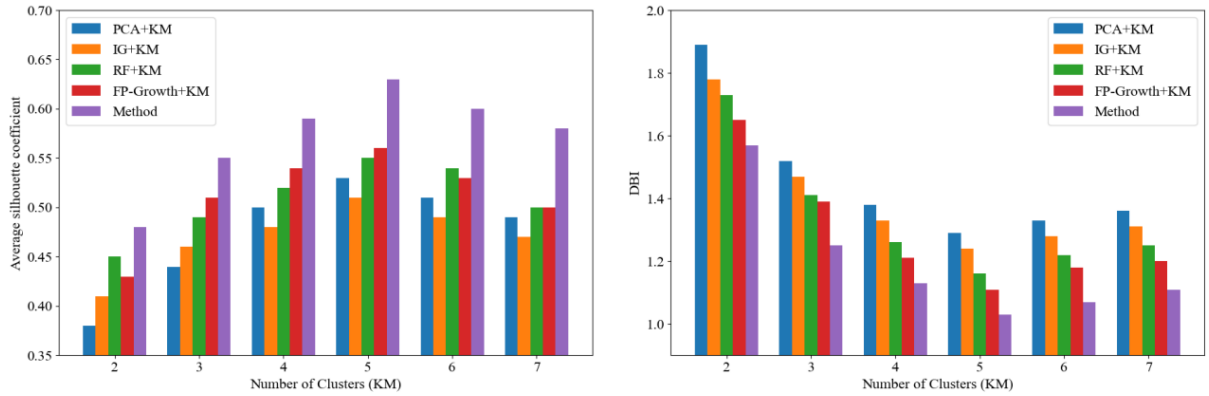

Figure 4: Performance evaluation of user preference clustering structures using different methods

In Figure 4, when the KM is 5, the silhouette coefficient of the proposed method reaches 0.63, 0.1 higher than the PCA solution. This gain is primarily due to the expressive power of the rule vector in the attribute combination dimension, enhancing the discriminability of user preference features. At the same KM value, the DBI drops to 1.03, significantly lower than IG's 1.24 and FP-Growth's 1.11. This is because the behavior-driven rule vector effectively eliminates redundant noise in some preference expressions, thereby compressing the fuzzy intervals of cluster boundaries. Except for the optimal point at KM of 5, the proposed method maintains high silhouette values and low separation index throughout the entire KM range from 3 to 7, demonstrating its robust ability to identify user preference structures. A larger silhouette coefficient value indicates a higher probability that a sample point is correctly assigned to the current cluster and a higher degree of differentiation from other clusters. Therefore, a higher silhouette coefficient indicates better clustering results. This demonstrates that the preference rule model constructed by this method effectively improves the stability and semantic consistency of cluster boundaries. Results show that the preference rule model, which co-encodes behavioral feedback and visual features, constructs a clear and separable user pattern structure within multi-cluster partitioning, effectively improving the stability and semantic consistency of cluster boundaries.

5.3 User satisfaction verification of the optimized design scheme

To further verify whether the perceived differences in recommended design solutions across different preference patterns exhibit structural consistency, this study categorizes user groups into five preference groups and constructs an evaluation system for group response consistency and recommendation acceptance rate. In the consistency analysis, the mean cosine similarity of ratings is used to measure the convergence of responses to the same recommended solution across users within a cluster, focusing on the model's ability to maintain group behavioral stability. The acceptance rate evaluation uses the proportion of users with scores higher than the preference threshold as an indicator to measure the effective adaptation of the recommendation scheme in the target preference group. The left sub-figure of Figure 5 shows the distribution differences of the consistency

scores of the above five methods in each cluster, and the right sub-figure shows the corresponding recommendation acceptance rate performance.

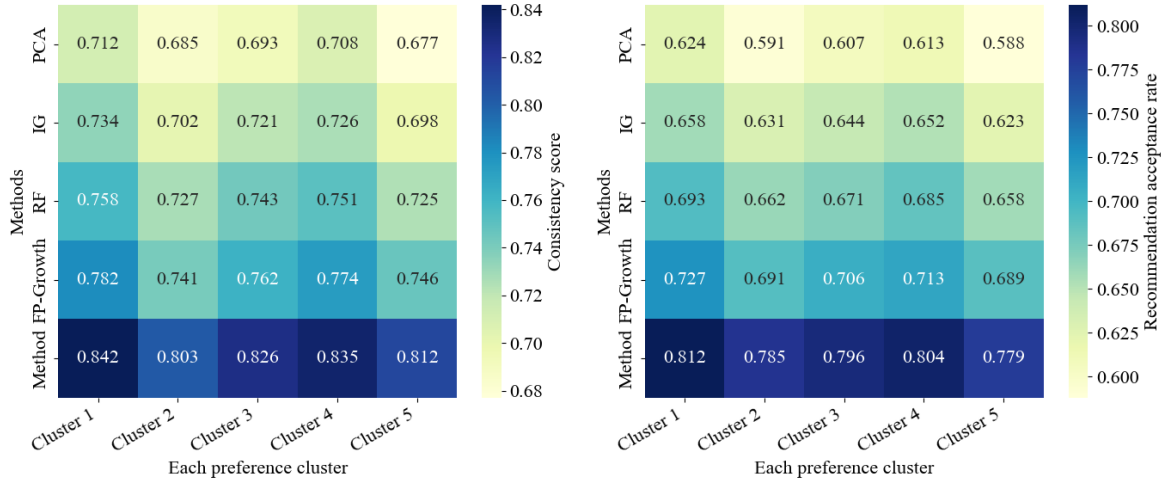

Figure 5: Comparison of design response consistency and acceptance rates of different methods in each preference group

In Figure 5, in terms of consistency scores, the proposed method achieves mean scores of 0.842 and 0.826 in Clusters 1 and 3, respectively. These scores are significantly higher than FP-Growth's scores of 0.782 and 0.762, and are 0.13 and 0.133 higher than the PCA method. This demonstrates that the preference modeling strategy based on the combination of visual element encoding and the Apriori rule is more effective in enhancing the expressive power of rating structures within a group. This advantage is not limited to a single cluster but is consistently demonstrated across all preference groups. In Clusters 2 and 4, the consistency score of this method is also higher than that of the other four methods, which are 0.803 and 0.835, respectively.

In the evaluation of recommendation acceptance rate, this method reaches 0.812 in Cluster 1, which is 0.085 and 0.119 higher than FP-Growth and RF, respectively, indicating that the recommended design scheme has a larger proportion of high-scoring feedback in this preference group, and the model output is closer to its explicit preference trend. In Cluster 5, FP-Growth and RF are close in value, but this method still leads with 0.779, indicating that it still has a robustness advantage in the boundary preference cluster. These results demonstrate that combining visual features with behavioral responses for rule-driven modeling significantly improves the consistency of rating structures and the strength of output acceptance within user clusters, validating this strategy's broad adaptability and structural stability for identifying preference patterns.

5.4 Comparative analysis of the distribution of visual elements in graphic designs after design optimization

To evaluate the actual impact of the optimization mechanism in improving the matching degree between visual structure and user preferences, this section conducts analysis based on the two dimensions of color distribution and layout structure, and compares the structural performance of the results generated by each method from the two aspects of the proportional difference of the visual main tone and the spatial offset of the typesetting center of gravity. At the color level, the average primary color ratio is used to measure the color balance of design samples under five main tones. The purpose is to examine whether the recommendation mechanism has color bias or concentration tendencies. The layout dimension uses the image center of gravity offset as a quantitative indicator of the balance of the layout structure, reflecting whether the optimization leads to the generation of a more visually stable layout composition. The dispersion of these offset values across all color categories is quantified by their interquartile range to assess structural consistency. The five color types represent different visual expression preferences. Cool blues are often used for rational and technological styles, while warm reds tend to be emotionally stimulating and visually impactful. Grayscale structures convey a simple and neutral visual tone; vibrant yellow has attention-directing properties; deep green is often associated with natural compositions. The left sub-figure in Figure 6 shows the average primary color proportions for each method under the five color categories, while the right sub-figure shows the distribution of layout offset values for the corresponding color samples.

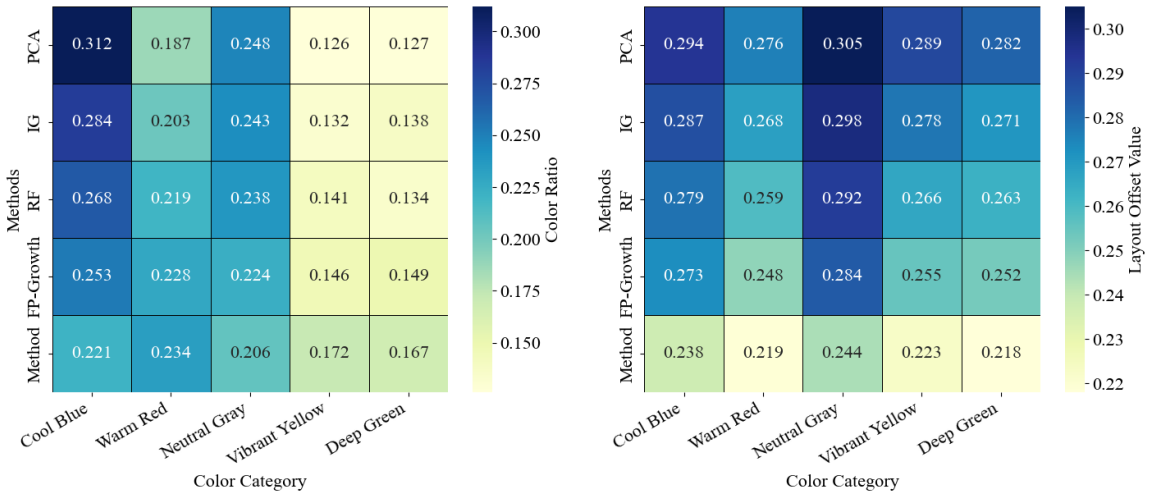

Figure 6: Multi-method comparison of visual dominant tone distribution and typographic structure shift in design optimization results

In Figure 6, both PCA and IG methods show a clear trend of cold blue dominance in the color structure distribution. The average dominant color ratio for this category in PCA is 0.312, significantly higher than that of other categories. This suggests that traditional dimensionality reduction strategies have not effectively suppressed color centralization in design solutions, and the lack of color diversity can lead to reduced preference matching accuracy. This method creates a more dispersed color structure across the five main tones. Vibrant yellow and deep green account for 0.172 and 0.167 of the totals, respectively, remaining within the low-skew range. Cool blue and warm red increase in their proportions to 0.221 and 0.234, respectively. This indicates that color selection behavior driven by high-confidence preference rules is aligned with user aesthetic intent, and the color matching strategy exhibits a clear trend toward harmony.

Regarding layout deviation, the proposed method is controlled at 0.244 or below in all color types, which is lower than the minimum deviation value of 0.248 of FP-Growth, and converges to 0.238 and 0.223 in the cold blue and vibrant yellow categories, respectively, showing the convergence enhancement effect of the layout structure in recommendation generation. The deviation values of the corresponding categories of the PCA method are 0.294 and 0.289, respectively, indicating that the problem of unstable layout structure has not been resolved. The results show that the optimization strategy based on preference rule constraints not only reduces the dominance of a single dominant tone at the color structure level but also improves the stability of the spatial composition, effectively supporting the output of preference consistency from the perspective of the input feature structure.

5.5 Testing model stability and preference generalization

In a multi-task design environment, to verify the cross-task adaptability of the preference modeling method in terms of maintaining structural rules and outputting results, it is necessary to examine its robustness and generalization capabilities under conditions of sample distribution changes. The stability evaluation uses the rule overlap rate as the core indicator to quantify the degree of intersection between the high-confidence rule sets extracted by each method in different tasks, reflecting the model's transferability at the rule structure level. The generalization ability is measured by the output consistency score, that is, the structural similarity between the recommended designs received by users with the same preferences in different tasks. This indicator focuses on evaluating the consistency of the recommendation mechanism in maintaining preferences. The five selected task scenarios encompass distinct design domains: commercial advertisements, publication covers, social platform content, data visualization interfaces, and brand identity design. Each task comprises an independent dataset of 256 samples with non-overlapping user groups, ensuring structural diversity and preventing cross-task bias. The left sub-graph in Figure 7 shows the average level of rule set overlap between different tasks for each method, and the right sub-graph depicts the consistency score of the output recommendation under the corresponding task.

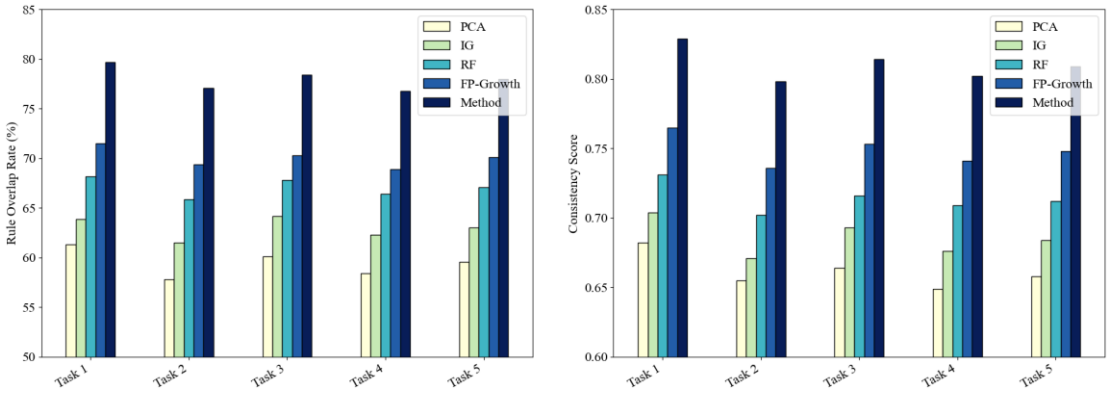

Figure 7: Comparison of different modeling methods in multi-task preference structure stability and recommendation output consistency

In Figure 7, in terms of rule structure stability, the proposed method achieves rule overlap rates of 79.7% and 78.4% in Tasks 1 and 3, respectively, which is higher than FP-Growth's 71.5% and 70.3%, a difference of over 8%, indicating that preference rules have greater structural scalability under task changes. This result stems from its user-behavior-driven multidimensional vector space construction, which improves the semantic consistency of rule generalization. In contrast, PCA achieves the lowest performance across all tasks, with an overlap rate of no more than 61.3%, indicating that its unsupervised compression-based feature set lacks structural consistency.

In terms of output consistency, the proposed method achieves scores of 0.798 on Task 2 and 0.809 on Task 5, respectively, exceeding FP-Growth by 0.062 and 0.061. This difference stems from the rule-driven generation mechanism's enhanced structural embedding of preference logic, resulting in output samples that more closely align with the user's original preference expression in terms of visual structure and dominant color distribution. The scores of IG and RF methods in Tasks 2 and 5 are concentrated between 0.671 and 0.712. The range of variation is limited by their policy frameworks that rely on local attribute contribution rates or conditional information and do not have the ability to express global preference structures. Experimental results show that the strategy of integrating user behavior responses with rule structures can effectively maintain the consistency of rule structures and the preference fit of recommendation outputs under task disturbance conditions, and has strong cross-scenario adaptability.

6 Discussion

This method demonstrates advantages over traditional modeling techniques in multidimensional evaluation. Its improved accuracy stems from a behavior-driven supervision mechanism that strengthens the semantic mapping between visual element combinations and user preferences during the rule generation phase, avoiding the loss of key perceptual information encountered in unsupervised dimensionality reduction by PCA. While FP-Growth achieves high recall at low support, its rule generalization is limited by its structural compression mechanism, resulting in a sharp decline in the size of the rule set at high support. This method constructs a user preference space by vectorizing rules, enabling K-means clustering to achieve a silhouette coefficient of 0.63, demonstrating greater internal consistency and clearer inter-cluster distinctions among the user groups it delineates. The optimized output achieves higher rating consistency and acceptance rates within each preference cluster, validating the effectiveness of embedding high-confidence rules as a constraint mechanism. In cross-task testing, both the rule overlap rate and output consistency score outperform comparable methods, demonstrating the greater adaptability of this modeling approach based on the collaborative encoding of behavioral feedback and multidimensional features. These performance advantages jointly confirm the effectiveness of this method's technical chain from feature encoding to rule mining to design optimization in solving the problems of user visual preference modeling and optimization in the field of graphic design.

7 Conclusions

This paper focuses on the accurate identification and optimization of user visual preferences in graphic design, and introduces a method that integrates feature encoding and Apriori rule mining. By constructing a multidimensional visual feature matrix including color, layout, font, and graphic structure, and combining user behavior feedback to generate standardized preference labels, the Apriori algorithm is used to extract high-confidence visual preference association rules. The rules are further vectorized and input into the KM clustering model to generate a preference pattern map of the user group. Finally, the rules are embedded as constraints in the automatic combination module of design elements to achieve personalized reconstruction of visual solutions and improve the consistency of output with user visual preferences. Experimental results show that the preference extraction accuracy of this method reaches 89.2% when the SC is 0.09, and the average silhouette coefficient reaches 0.63 when the number of clusters is 5, verifying its effectiveness and adaptability in preference modeling and design optimization. The experimental validation demonstrates superior performance compared to

alternative feature modeling and rule extraction techniques, affirming the method's advancement in achieving precise and interpretable visual preference recognition for targeted design optimization.

This study relies on behavioral data collected from specific regions to model user preferences, whose cultural background and aesthetic preferences may affect the universality of the rules. The constructed feature encoding system does not include dynamic interactions or three-dimensional visual elements, limiting the model's adaptability to complex scenarios. The current optimization mechanism is based on deterministic rule constraints and has not yet integrated generative architectures to explore a richer design space. Future work can expand the diversity of data sources, introduce multimodal perception dimensions, and explore the semantic embedding capabilities of neural network structures in layout generation to improve the system's response accuracy and output diversity to unstructured preferences.

Funding

This work was supported by project ofResearch on Design Inspiration in the Field of Special Engineering Equipment for the Digital Intelligence Era", the Director's Research Fund of the Guangxi Key Laboratory of Special Engineering Equipment and Control for the year 2024.(No.SEEC24ZR07)

References

[1] H. Xie, “Analysis of interaction function of modern graphic design based on technical-aided design,” *Journal of King Saud University-Science*, Elsevier, vol. 35, no. 8, p. 102828, 2023. https://doi.org/10.1016/j.jksus.2023.102828

[2] B. Matthews, B. Shannon, and M. Roxburgh, “Destroy all humans: the dematerialisation of the designer in an age of automation and its impact on graphic design—a literature review,” *International Journal of Art & Design Education*, Wiley Online Library, vol. 42, no. 3, pp. 367–383, 2023. https://doi.org/10.1111/jade.12460

[3] Y. Shi, T. Gao, X. Jiao, and N. Cao, “Understanding design collaboration between designers and artificial intelligence: a systematic literature review,” *Proc ACM Hum Comput Interact*, ACM, vol. 7, no. CSCW2, pp. 1–35, 2023. https://doi.org/10.1145/3610217

[4] Z. Wang, “Aesthetic evaluation of multidimensional graphic design based on voice perception model and internet of things,” *International Journal of System Assurance Engineering and Management*, Springer, vol. 13, no. 3, pp. 1485–1496, 2022. https://doi.org/10.1007/s13198-021-01492-2

[5] W. Zhu, “A Study of Big-Data-Driven Data Visualization and Visual Communication Design Patterns,” *Sci Program*, Wiley Online Library, vol. 2021, no. 1, p. 6704937–6704947, 2021. https://doi.org/10.1155/2021/6704937

[6] Y. Dong, S. Zhu, and W. Li, “Promoting sustainable creativity: An empirical study on the application of mind mapping tools in graphic design education,” *Sustainability*, MDPI, vol. 13, no. 10, p. 5373, 2021. https://doi.org/10.3390/su13105373

[7] Q. Liu *et al.*, “Multimodal recommender systems: A survey,” *ACM Comput Surv*, ACM, vol. 57, no. 2, pp. 1–17, 2024. https://doi.org/10.1145/3695461

[8] F. Lei, Z. Cao, Y. Yang, Y. Ding, and C. Zhang, “Learning the user’s deeper preferences for multi-modal recommendation systems,” *ACM Transactions on Multimedia Computing, Communications and Applications*, ACM, vol. 19, no. 3s, pp. 1–18, 2023. https://doi.org/10.1145/3573010

[9] M. Li, Z. Zhang, and T. Lin, “Streamlining Visual UI Design: Mining UI Design Patterns for Top App Bars,” *Applied Sciences*, MDPI, vol. 15, no. 3, p. 1060, 2025. https://doi.org/10.3390/app15031060

[10] A. Chatzimparmpas, R. M. Martins, and A. Kerren, “VisRuler: Visual analytics for extracting decision rules from bagged and boosted decision trees,” *Inf Vis*, Sage Publications, vol. 22, no. 2, pp. 115–139, 2023. https://doi.org/10.1177/14738716221142005

[11] A. Alvarez, J. Font, and J. Togelius, “Toward designer modeling through design style clustering,” *IEEE Trans Games*, IEEE, vol. 14, no. 4, pp. 676–686, 2022. https://doi.org/10.1109/TG.2022.3143800

[12] J. Rezwana and M. Lou Maher, “Designing creative AI partners with COFI: A framework for modeling interaction in human-AI co-creative systems,” *ACM Transactions on Computer-Human Interaction*, ACM, vol. 30, no. 5, pp. 1–28, 2023. https://doi.org/10.1145/3519026

[13] Z. Pan, H. Pan, and J. Zhang, “The application of graphic language personalized emotion in graphic design,” *Heliyon*, Cell, vol. 10, no. 9, 2024. https://www.cell.com/heliyon/fulltext/S2405-8440(24)06211-X

[14] W. Kong *et al.*, “Aesthetics++: Refining graphic designs by exploring design principles and human preference,” *IEEE Trans Vis Comput Graph*, IEEE, vol. 29, no. 6, pp. 3093–3104, 2022. https://doi.org/10.1109/TVCG.2022.3151617

[15] R. S. Gbadegbe, J. Amewu, E. Krampa, and S. N. A. Sampah, “Analysis of factors that influence graphic design as the preferred visual art subject in Ghana,” *Cogent Education*, Taylor & Francis, vol. 11, no. 1, p. 2423604, 2024. https://doi.org/10.1080/2331186X.2024.2423604

[16] S. Liao, R. Widowati, and C. Y. Lee, “Data mining analytics investigation on TikTok users' behaviors: social media app development,”

Library Hi Tech, vol. 42, no. 4, pp. 1116–1131, 2024.https://doi.org/10.1108/LHT-08-2022-0368

[17] Y. Li, C. Zhang, J. Li, and et al., "MCoR-Miner: Maximal co-occurrence nonoverlapping sequential rule mining," IEEE Transactions on Knowledge and Data Engineering, vol. 35, no. 9, pp. 9531–9546, 2023. https://doi.org/10.1109/TKDE.2023.3241213

[18] E. Akgül, Y. Delice, E. K. Aydoğan, and F. E. Boran, "An application of fuzzy linguistic summarization and fuzzy association rule mining to Kansei Engineering: a case study on cradle design," *J Ambient Intell Humaniz Comput*, Springer, vol. 13, no. 5, pp. 2533–2563, 2022. https://doi.org/10.1007/s12652-021-03292-9

[19] T. Kusnandar, J. Santoso, and K. Surendro, "Enhancing Color Selection in HSV Color Space," *Ingenierie des Systemes d'Information*, ProQuest, vol. 29, no. 4, p. 1483, 2024. DOI:10.18280/isi.290421

[20] H. Kim, H. Lee, S. Ahn, W.-K. Jung, and S.-H. Ahn, "Broken stitch detection system for industrial sewing machines using HSV color space and image processing techniques," *J Comput Des Eng*, Oxford Academic, vol. 10, no. 4, pp. 1602–1614, 2023. https://doi.org/10.1093/jcde/qwad069

[21] P. Doungmala and T. H. Thai, "Investigation into the application of image modeling technology in the field of computer graphics," *International Journal for Applied Information Management*, ijaim, vol. 3, no. 2, pp. 82–90, 2023. https://doi.org/10.47738/ijaim.v3i2.53

[22] F. Wang, C. Wang, and Q. Guan, "Single-shot fringe projection profilometry based on deep learning and computer graphics," *Opt Express*, OPTICA, vol. 29, no. 6, pp. 8024–8040, 2021. https://opg.optica.org/oe/fulltext.cfm?uri=oe-29-6-8024&id=448672

[23] A. Lewandowska, A. Olejnik-Krugly, J. Jankowski, and M. Dziśko, "Subjective and objective user behavior disparity: Towards balanced visual design and color adjustment," *Sensors*, MDPI, vol. 21, no. 24, p. 8502, 2021. https://doi.org/10.3390/s21248502

[24] A. G. Martín, A. Fernández-Isabel, I. Martín de Diego, and M. Beltrán, "A survey for user behavior analysis based on machine learning techniques: current models and applications," *Applied Intelligence*, Springer, vol. 51, no. 8, pp. 6029–6055, 2021. https://doi.org/10.1007/s10489-020-02160-x

[25] L. Zhu *et al.*, "An active service recommendation model for multi-source remote sensing information using fusion of attention and multi-perspective," *Remote Sens (Basel)*, MDPI, vol. 15, no. 10, p. 2564, 2023. https://doi.org/10.3390/rs15102564

[26] X. Zhao, L. Lin, X. Guo, Z. Wang, and R. Li, "Evaluation of Rural Visual Landscape Quality Based on Multi-Source Affective Computing," *Applied Sciences*, MDPI, vol. 15, no. 9, p. 4905, 2025. https://doi.org/10.3390/app15094905

[27] Zhou M, Zhang J, Adomavicius G. Longitudinal impact of preference biases on recommender systems' performance[J]. Information Systems Research, 2024, 35(4): 1634-1656.https://doi.org/10.1287/isre.2021.0133

[28] H. Xie, "Research and case analysis of apriori algorithm based on mining frequent item-sets," *Open J Soc Sci*, scirp, vol. 9, no. 04, p. 458, 2021. http://www.scirp.org/journal/Paperabs.aspx?PaperID=108829

[29] S. Sharma, L. Koehl, P. Bruniaux, X. Zeng, and Z. Wang, "Development of an intelligent data-driven system to recommend personalized fashion design solutions," *Sensors*, MDPI, vol. 21, no. 12, p. 4239, 2021. https://doi.org/10.3390/s21124239

[30] M. Kaushik, R. Sharma, S. A. Peious, M. Shahin, S. Ben Yahia, and D. Draheim, "A systematic assessment of numerical association rule mining methods," *SN Comput Sci*, Springer, vol. 2, no. 5, p. 348, 2021. https://doi.org/10.1007/s42979-021-00725-2